Available online at www.sciencedirect.com
SCIENCE DIRECT®
Journal of Crystal Growth 255 (2003) 258–265
JOURNAL OF CRYSTAL GROWTH
www.elsevier.com/locate/jcrysgro

Origin of photoluminescence of GaAsN/GaN(0 0 1) layers grown by plasma-assisted solid source molecular beam epitaxy

S.Z. Wang[a,*], S.F. Yoon[a], W.K. Loke[a], C.Y. Liu[b], S. Yuan[b]

[a] *Singapore-Massachusetts Institute of Technology (MIT) Alliance, School of Electrical and Electronic Engineering, Nanyang Technological University, Nanyang Avenue, Singapore 639798, Singapore*

[b] *School of Materials Engineering, Nanyang Technological University, Nanyang Avenue, Singapore 639798, Singapore*

Received 15 March 2003; accepted 3 April 2003
Communicated by M. Schieber

Abstract

This paper reports the low temperature photoluminescence (PL) characteristics of GaAsN grown by radio frequency nitrogen plasma-assisted solid source molecular beam epitaxy. It is found that the PL peak of GaAsN at low temperature is not originated from band-to-band transitions, but from localized exciton recombinations, even though the GaAsN material is of good crystalline quality as verified by reflection high-energy electron diffraction and X-ray diffraction measurements. The interstitial N–As complex and defects related to the broad low energy-tail in the PL spectrum could be effectively removed by thermal annealing. The red-shift in the PL peak of GaAsN after annealing is to the best of our knowledge reported for the first time. This phenomenon depends on the growth conditions, in particular the nitrogen flux. The red-shift in the PL peak energy is useful for extending the GaAs-based nitride material to long wavelength applications. It is also noticeable that the full-width at half maximum of PL peak from GaAsN decreases linearly with the increasing annealing temperatures.
© 2003 Elsevier Science B.V. All rights reserved.

PACS: 78.55.Cr; 81.05.Ea; 81.15.Hi

Keywords: A1. Characterization; A3. Molecular beam epitaxy; B1. Nitrides

1. Introduction

GaAs-based Ga(In)AsN materials are attracting a great level of attention due to their useful physical properties for a wide range of potential optoelectronic applications. Although GaAs-based Ga(In)AsN semiconductor lasers emitting in the communication wavelength windows of 1.3 and 1.55 μm have been demonstrated [1,2], the physical origin of the extremely large bowing parameter remains unclear. For example, the bowing parameter of GaAsN could reach more than 20 eV [3,4], compared with the bowing parameters of 0.4 eV for AlGaAs, 0.46 eV for InGaAs, 1.1 eV for GaAsSb, and 0.2 eV for GaAsP [5]. The premise for accurate determination of the bowing parameter is to clearly identify

*Corresponding author.
E-mail address: szwang@ntu.edu.sg (S.Z. Wang).

0022-0248/03/$ - see front matter © 2003 Elsevier Science B.V. All rights reserved.
doi:10.1016/S0022-0248(03)01265-X

the band-edge of GaAsN. Unfortunately, the existence of localized states makes it somewhat difficult to accurately identify the band-edge. The different experimental methods used to determine the bowing parameter, including photoluminescence (PL) and absorption spectrum result in differences in understanding the band-edge of GaAsN materials.

In this paper, we report PL experiments on GaAsN that reveal its PL origin at low temperature. It was found that the PL from GaAsN does not originate from band-to-band transitions, but rather from localized state excitonic recombinations, even in samples of high crystalline quality. To the best of our knowledge, our results show for the first time the existence of red-shift in the PL peak energy after thermal annealing, which could serve a useful purpose of extending the GaAsN material to long wavelength emission. The interstitial N–As complex and the defects related to the broad energy-tail in the low-energy side of the PL spectrum could be effectively removed by thermal annealing process.

2. Experimental conditions

The GaAsN samples were grown by radio frequency (RF) nitrogen plasma-assisted solid-source molecular beam epitaxy (SSMBE). The growth chamber is equipped with standard effusion cells for group III elements and valved cracker cells for arsenic and phosphorus. The active nitrogen species are supplied by a RF nitrogen plasma source. All samples were grown on (0 0 1)-oriented semi-insulating (SI) GaAs substrates, prepared following standard procedures. Prior to growth, surface oxide desorption was carried out under As flux at beam equivalent pressure (BEP) of 6.2×10^{-6} Torr. (2×4) surface reconstruction was maintained throughout the entire growth process. The BEPs for Ga and As were 4.5×10^{-7} and 6.2×10^{-6} Torr, respectively. The As/Ga flux ratio was fixed at about 14. The growth rate was $\sim1.0\,\mu$m/h, verified by time-resolved reflection high-energy electron diffraction (RHEED) measurements and X-ray diffraction (XRD) measurements. The nitrogen plasma source works optimally at nitrogen background pressure of 1.0×10^{-5} Torr in the presence of BEP_{As} of 6.2×10^{-6} Torr, and is activated by RF power greater than 60 W to maintain the plasma in high brightness mode.

An undoped GaAs buffer layer of ~300 nm was first grown on the GaAs substrate at 590°C. The substrate temperature was then reduced to 460°C for the growth of GaAsN epilayer. The thickness of the GaAsN layer was ~100 nm, followed by a 20 nm-thick GaAs cap layer. XRD measurements were carried out to check the GaAsN crystalline quality. PL measurements were performed at 5 K. Excitation was at near normal incidence using the 514.5 nm line from an Ar ion laser. The PL signals were collected with a dual-grating spectrometer in the reflection direction and detected using a liquid-nitrogen cooled germanium (Ge) detector in association with a standard lock-in technique.

3. Results and discussion

3.1. Physical origins for PL peaks

Fig. 1 shows an XRD rocking curve of the GaAsN sample for (0 0 4) diffraction. The solid

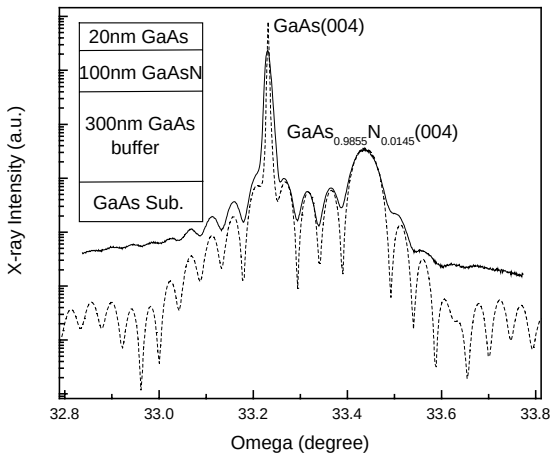

Fig. 1. A XRD rocking curve of an as-grown GaAsN sample for the (0 0 4) diffraction direction. The sample structure is illustrated in the inset. The solid curve is the experimental data, and the dashed curve is a simulation result using the dynamic theory.

curve is experimental data, and the dashed curve is an optimal simulation result based on dynamical theory. The simulation result is in close agreement with the experimental data. With reference to the GaAs substrate peak, the GaAsN peak is easily identifiable, and the nitrogen composition deduced from the simulation is 1.45%. Consistent with the RHEED pattern observation, the strong XRD peak testifies to the high crystalline quality of the $GaAs_{0.9855}N_{0.0145}$ epilayer. Strong Pendellosung fringes are observed in the XRD spectrum, indicating the presence of a smooth and abrupt $GaAs_{0.9855}N_{0.0145}$/GaAs interface.

Fig. 2 shows a PL spectrum (solid circles) of the $GaAs_{0.9855}N_{0.0145}$ epilayer at 5 K. The PL spectrum is characterized by a twin structure located at 1.224 and 1.202 eV, respectively. A broad bandtail extends for several tens of meV into the low-energy side of the PL spectrum. Using the bowing coefficient C of 18.5 eV for $GaAs_{0.9855}N_{0.0145}$ material reported in Ref. [4], the bandgap of $GaAs_{1-x}N_x$ can be calculated from

$$E_g(GaAs_{1-x}N_x) = (1-x)E_g(GaAs) + xE_g(GaN) - x(1-x)C, \quad (1)$$

where x denotes the nitrogen composition in $GaAs_{1-x}N_x$, and $E_g(GaAs_{1-x}N_x)$ is the bandgap

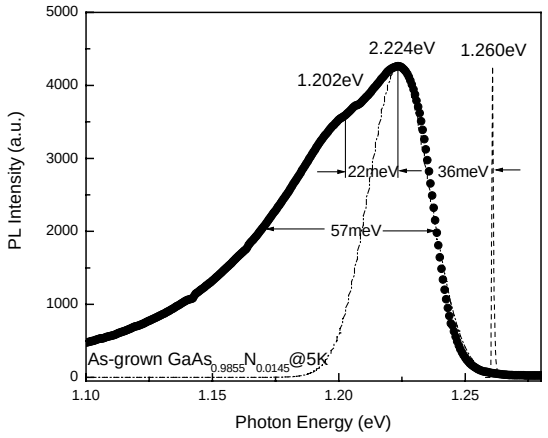

Fig. 2. A PL spectrum from the as-grown $GaAs_{0.9855}N_{0.0145}$ sample at 5 K. The solid circles are the experimental data. The dashed curve is a theoretical PL peak due to the band-to-band transition of the $GaAs_{0.9855}N_{0.0145}$ sample at 5 K. The dash-dotted curve is a calculated recombination of the excitons at the localized states.

of $GaAs_{1-x}N_x$. E_g(GaAs) is the bandgap of GaAs, and E_g(GaN) the bandgap of the zinc-blende structure GaN. C is the bowing coefficient for GaAsN. However, the bowing coefficient reported in Ref. [4] was obtained at room temperature. Therefore, Eq. (1) can only be used to calculate the $GaAs_{1-x}N_x$ bandgap at room temperature. The bandgap dependence on temperature is reported in Ref. [6], and is given by

$$E_g(T) = E_g(RT) + \frac{\alpha(RT)^2}{RT+\beta} - \frac{\alpha T^2}{T+\beta}, \quad (2)$$

where $E_g(T)$ is the bandgap of $GaAs_{1-x}N_x$ at temperature T, and $E_g(RT)$ the bandgap of $GaAs_{1-x}N_x$ at room temperature. The values of α and β is 5.5×10^{-4} eV/K and 370 K, respectively [6]. The PL peak due to band-to-band transitions can then be calculated using

$$I_{bb} = A_{bb}(\hbar\omega)^2(\hbar\omega - E_g)\exp\left(-\frac{\hbar\omega - E_g}{k_B T}\right) \quad (3)$$

I_{bb} is the PL intensity due to band-to-band transitions, and $\hbar$ is Planck's constant. ω is the angular frequency of emission, E_g the bandgap of $GaAs_{1-x}N_x$, and k_B the Boltzmann's constant. A_{bb} is a fitting parameter for the PL intensity. The calculated PL peak due to band-to-band transitions in $GaAs_{0.9855}N_{0.0145}$ at 5 K is then shown in Fig. 2 as the dashed curve peak at 1.260 eV. The energy difference between the calculated band-to-band emission peak and the experimental PL peak suggests that the PL peak at 1.224 eV does not originate from band-to-band transitions in the $GaAs_{0.9855}N_{0.0145}$ sample, due to (i) there is a 36 meV energy separation between the calculated band-edge recombination and measured PL peak, (ii) the calculated band-edge emission is only $\sim$0.08 meV in half-width, while the measured PL peak has much wider half-width (57 meV), (iii) the increasing trend in the high-energy side of the calculated 1.260 eV peak and the measured 1.224 eV peak is fundamentally different, that suggests they may originate from different physical origins. Therefore, it might be improper to consider the measured 1.224 eV PL peak as the energygap of the $GaAs_{1-x}N_x$ sample. In the most common cases, the intrinsic emission in pure semiconductors at low temperature is often due

to the excitonic recombination. It is known that the exciton binding energy in GaAs is 4.2 meV [7], and the value in GaN is ~20 meV [8]. Because of the relatively low nitrogen composition (~1.45%) in our $GaAs_{0.9855}N_{0.0145}$ sample, the exciton binding energy can be approximated using linear interpolation between the exciton binding energies of GaAs and GaN. Using such interpolation, the exciton binding energy of our $GaAs_{0.9855}N_{0.0145}$ sample is estimated to be 4.4 meV. This value is far smaller than the 36 meV energy separation between the calculated band-edge recombination and measured PL peak. Hence, it is highly unlikely that the 1.224 eV PL peak originates from the free exciton recombination. According to a report by Kaschner et al. [9], the 1.224 eV PL peak is ascribed to the recombination of localized excitons. Nitrogen-related localized states have been reported by Grenouillet et al. [10]. Taking the localized states into consideration, the energy of an emitted photon is therefore given by

$$\hbar\omega = E_g - (E_b + E_{LX}), \tag{4}$$

where $\hbar$ is Planck's constant, ω the angular frequency of emission, and E_g the bandgap of $GaAs_{1-x}N_x$. E_b denotes the exciton binding energy of the $GaAs_{1-x}N_x$ sample, and E_{LX} the energy level of the localized state. Based on this, the calculated energy level of the localized state is 31.6 meV. The dash-dotted curve in Fig. 2 is a calculated PL emission spectrum due to recombination of localized excitons I_{ex} weighted by the following Gaussian function profiles [11], with the 31.6 meV localization energy taken into account

$$I_{ex} = A_{ex}\exp\left(-\frac{[\hbar\omega - E_{ex}(T)]^2}{2\sigma_{ex}^2(T)}\right)\exp\left(-\frac{\hbar\omega}{k_B T}\right), \tag{5}$$

where A_{ex}, E_{ex} and σ_{ex} are the amplitude, energy, and broadening parameters of the localized state exciton recombination. The tail at low-energy side of the measured PL spectrum extends for several tens of meV from the calculated localized exciton recombination emission spectrum, in contrast to the excellent agreement at high-energy side of the PL spectrum. Therefore, other recombination mechanisms have to be considered to account for the deviation at the low-energy side of the PL spectrum, and this aspect warrants further investigation.

The presence of nitrogen-related defects has been cited as a possible reason for the low-energy tail in the PL spectrum [12]. We further reported that one of the nitrogen-related defects was the interstitial N–As complex in the $GaAs_{1-x}N_x$ lattice [13]. It is possible that the excitons could be located at such interstitial N–As complexes at low temperature, and its recombination at these complexes could result in the shoulder peak or energy tail in the measured PL spectrum. The interstitial N–As complexes could be removed by thermal treatment through processes such as "kick-out" and out-diffusion, and thereafter the relevant PL peak would disappear. The 1.202 eV PL peak does disappear after annealing, as is in good agreement with the annealing behavior of the interstitial N–As complex. Hence, it is reasonable to relate the 1.202 eV PL peak to the interstitial N–As complexes. Further evidence for this will be provided in subsequent parts of this paper.

3.2. Localization energy in $GaAs_{1-x}N_x$ alloy

The localization energy of ~31.6 meV in the $GaAs_{0.9855}N_{0.0145}$ sample is much higher than that in other semiconductor materials. For example, the localization energies of $Zn_{0.97}Hg_{0.03}Te$, $CdS_{0.36}Se_{0.64}$ and $Cd_{0.92}Hg_{0.08}Te$ are as small as 4.8, 4.3 and 6.5 meV, respectively. The localization energy E_{LX} could be understood in the frame of the random distribution of the constituent atoms in crystal lattice [14].

$$E_{LX} = \eta[x(1-x)]^{2/3}\left(\frac{dE_g}{dx}\right)^2, \tag{6}$$

where η is a material-related proportional constant, x denotes the alloy composition, and dE_g/dx is the energygap derivative of the alloy over its composition, as is obtained from Eq. (1).

$$\frac{dE_{g(AB_{1-x}C_x)}}{dx} = E_{g(AC)} - E_{g(AB)} - C + 2Cx. \tag{7}$$

As a comparison, the energygap derivatives of GaAsN and CdSSe over their compositions are calculated in Table 1. The bowing coefficient for CdSSe alloy is experimentally obtained as 0.54 eV

[15]. dE_g/dx for GaAsN is therefore much greater than that for CdSSe. Differing from other semiconductor alloys whose energygaps follow the composition almost linearly, GaAsN alloy has an energygap strongly composition-dependent. Fig. 3a shows localization energies for GaAsN alloys as a function of the nitrogen composition. Solid circles represent the experimental data. The curve is a best fit using Eqs. (6) and (7), and is valid for the nitrogen content less than 3.5%, since the available values of bowing parameter C in Eq. (7) merely reach the nitrogen limit in GaAsN of around 3.5% [4]. While for CdSSe alloy, the bowing parameter C is approximately composition-independent. The calculated values are therefore valid in the whole composition range, as is shown in Fig. 3b where the solid square is an experimental datum. The localization energy in GaAsN alloy is at least one-order higher than that in CdSSe alloy, which is believed to be a typical sample amongst other II–VI and III–V semiconductor alloys since their bowing coefficients are usually small and approximately composition-independent.

Table 1
A comparison of the energygap derivative over alloy composition for GaAsN and CdSSe

	$GaAs_{0.9855}N_{0.0145}$	$CdS_{0.36}Se_{0.64}$
$\frac{dE_{g(AB_{1-x}C_x)}}{dx}$ (eV)	−16.1457	−0.6388

3.3. Anneal effects on PL property

Fig. 4 shows a 5 K PL spectrum of the $GaAs_{0.9855}N_{0.0145}$ sample (same sample as in Fig. 2), which has been subjected to 10 min of thermal annealing at 800°C. The solid circles are experimental data, and the dash-dotted curve is a best fit obtained using Eq. (5). The significant low-energy tail present in the PL spectrum of the as-grown $GaAs_{0.9855}N_{0.0145}$ sample is greatly suppressed after thermal annealing. This suggests that most of the nitrogen-related defects, including the interstitial N–As complexes described previously, were effectively annihilated by the annealing processes. This explains the significant suppression of the PL peak related to the interstitial N–As complexes after annealing. However Grenouillet et al. reported that the localized states could not be effectively removed by the annealing process [10]. That is because the presence of localized states is the intrinsic property of a ternary alloy according to the implication of Eq. (6). Therefore, the PL emission from the annealed $GaAs_{0.9855}N_{0.0145}$ sample could predominantly be due to localized state exciton recombination, as is testified by the good agreement between the calculated

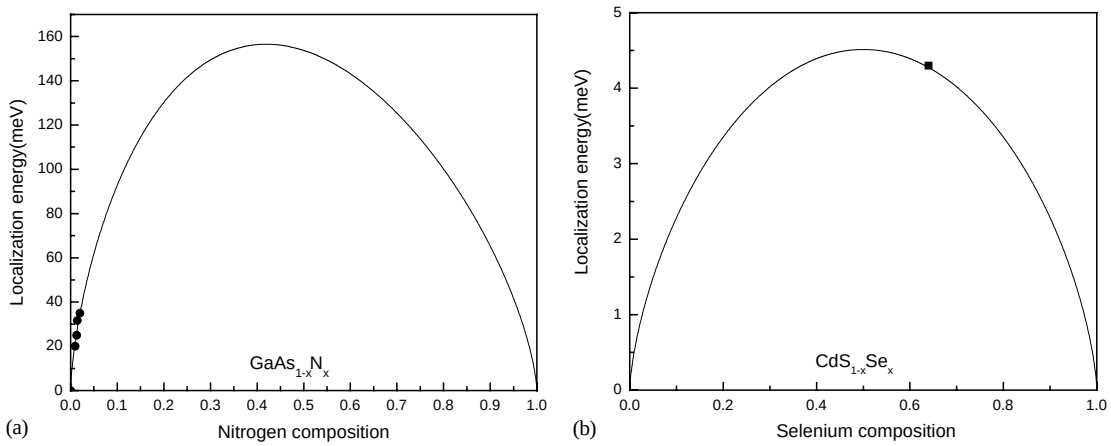

Fig. 3. A comparison of localization energies between GaAsN alloy and CdSSe alloy. The solid circles (Fig. 3a) and square (Fig. 3b) are experimental data, and the solid curves are obtained by fitting the random distribution model to the experimental results.

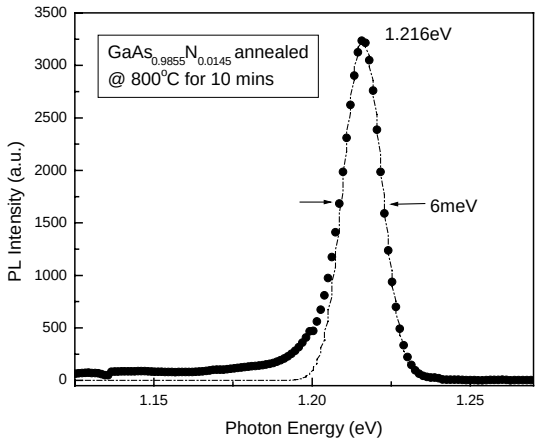

Fig. 4. A low temperature PL spectrum from the $GaAs_{0.9855}N_{0.0145}$ sample annealed at 800°C for 10 min. The solid circles are the experimental data. The dash-dotted curve is a calculated recombination of the excitons at the localized states.

localized-exciton recombination and the measured PL spectrum.

Fig. 5 shows the PL spectra of the $GaAs_{0.9855}N_{0.0145}$ sample (same sample as in Figs. 2 and 4) annealed for 10 min at different temperatures. Following the increase in the annealing temperature from 600°C to 650°C, the low-energy shoulder peak in the PL spectrum disappeared promptly due to removal of the interstitial N–As complexes, while the width of the PL peak is significantly suppressed only at higher annealing temperatures approaching 800°C. This could suggest that the thermal activation energy of the interstitial N–As complexes is lower than that of other defects. The increase in annealing temperature results in significant reduction in the full-width at half-magnitude (FWHM) of the PL spectrum from 57 to 6 meV. Correspondingly, the intensity of the PL spectrum is increased, indicating significant improvement in optical quality of the $GaAs_{0.9855}N_{0.0145}$ sample. It is interesting to note in Fig. 6 that the main PL peak exhibited a red-shift of 18 meV from 1.234 to 1.216 eV following the increase in annealing temperature while our previous experiments have shown that the PL peak of $GaAs_{0.981}N_{0.019}$ bulk layer blue-shifted by 75 meV from 0.948 eV (as-grown sample) to 1.023 eV after being annealed at

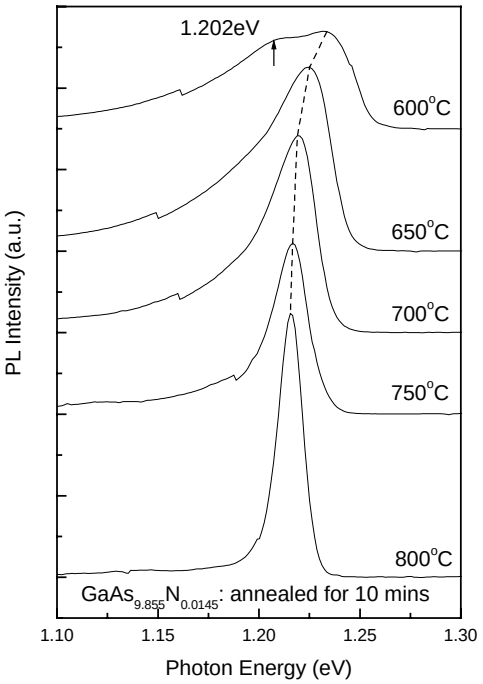

Fig. 5. The low temperature PL spectra of a batch of $GaAs_{0.9855}N_{0.0145}$ samples annealed for 10 min at different temperatures. It is evident that the shoulder peak at 1.202 eV disappeared after annealing and the main peak redshifts following the annealing temperatures.

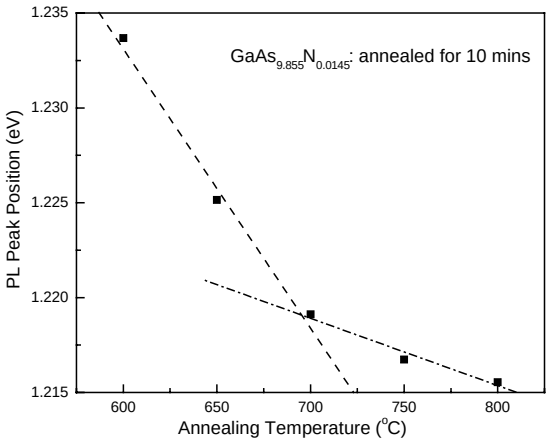

Fig. 6. A relationship between the low-temperature PL peak position and the annealing temperature.

750°C for 10 min [12]. Checking with the growth conditions for the $GaAs_{0.981}N_{0.019}$ and $GaAs_{0.9855}N_{0.0145}$ epilayers, the difference lies in

that the N_2 background pressure for the $GaAs_{0.981}N_{0.019}$ sample is 3.6×10^{-6} Torr with high RF power and for the $GaAs_{0.9855}N_{0.0145}$ sample is 1.0×10^{-5} Torr with low RF power. The use of larger nitrogen flux (with low RF power) could result in greater amount of interstitial N–As complexes, which could act as an effective source of nitrogen to hop into the $GaAs_{1-x}N_x$ lattice through "kick-out" mechanism when the $GaAs_{1-x}N_x$ sample undergoes the annealing process [16]. Such an effect could increase the nitrogen composition in the $GaAs_{1-x}N_x$ sample and give rise to a red-shift in the PL peak. The red-shift in the PL peak energy could be a useful effect for extending GaAs-based nitrides to long wavelength applications.

Fig. 6 shows the relationship between the PL peak position and annealing temperature. At temperatures below 700°C, the rate of reduction in the PL peak energy is apparently larger than the rate of reduction above 700°C. The rapid red-shift of the PL peak happens around 650°C (from 600°C to 700°C), and then slow down at annealing temperatures higher than 700°C (from 700°C to 800°C). The annealing temperature span for the rapid red-shift of the PL peak is in accordance with the temperature region in which the 1.202 eV shoulder peak vanishes. It is reasonable to consider that the rapid red-shift is related to the 1.202 eV peak. The 1.202 eV PL peak has been previously in this paper related to the interstitial N–As complexes. Therefore, here again shown a clue that the red-shift effect is due to the nitrogen source dissociated from the interstitial N–As complexes hopping into the GaAsN lattice by the so-called "kick-out" process. When the annealing temperature increases further higher than 700°C, the "kick-out" process becomes gentler because of the reduction on the concentration of the N–As interstitial complex due to the consumption of the N–As interstitial complex under lower annealing temperatures. That results in the saturation behavior of the movement of the PL peak.

Fig. 7 shows the FWHM of measured PL peak as a function of annealing temperature. It is noticeable that the FWHM decreases linearly following the annealing temperatures. In a common sense, the PL peak broadens through several

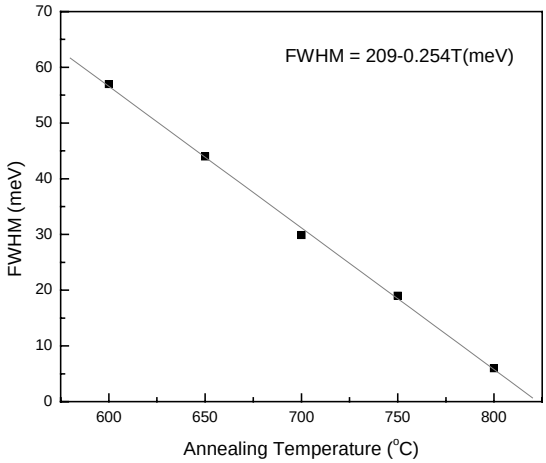

Fig. 7. The FWHM of measured PL peak is shown as a function of the annealing temperature.

mechanisms as nitrogen random distribution, local lattice distortion around nitrogen atoms, and material nonuniformity [17]. However, the random distribution of nitrogen atom is an intrinsic property for GaAsN alloy. We suppose the degree of N-induced lattice distortion and material nonuniformity decreases linearly with the increasing annealing temperature, that is, the FWHM decreases linearly with the annealing temperature

$$\mathrm{FWHM} = \mathrm{FWHM}_0 + \alpha_0 T. \quad (8)$$

The solid squares in Fig. 7 are experimental data, and the solid line is a best fit to these experimental data using Eq. (8), with FWHM_0 and α_0 equaling to 209 meV and –0.254 meV mol-percentage^{-1}, respectively. Then we have

$$\mathrm{FWHM} = 209 - 0.254\ \mathrm{T}(600^\circ\mathrm{C} \leqslant T \leqslant 800^\circ\mathrm{C}). \quad (9)$$

4. Conclusions

In summary, our experiments revealed that the PL peak of GaAsN at low temperature did not originate from the band-to-band transition, but from the recombination of exciton located at localized states, even though the GaAsN sample is of good crystalline quality verified by both RHEED observations and XRD measurements.

The emissions from localized excitons are intrinsic property of semiconductor alloys, and thus are very important to the research subjects relative to alloys' energyband. The interstitial N–As complex and the defects related to the broad energy-tail in the low-energy side of the PL spectrum could be effectively removed by thermal annealing process. Redshift phenomenon of the PL peak is to our knowledge firstly found in GaAsN material after annealing. However, this phenomenon strictly depends on the growth condition, especially on the nitrogen flux. In contrast to the blueshift due to annealing, the redshift is a useful phenomenon for the GaAs-based nitrides to extend to longer wavelength. It is also noticeable that the FWHM of PL peak from GaAsN decreases linearly with the increasing annealing temperatures.

Acknowledgements

One (S.Z. Wang) of the authors would like to express his appreciations to Mr. T.K. Ng and Dr. Z.Z. Sun for their helps during material growth and ex situ rapid thermal treatment, and to Dr. W.J. Fan for inspirational discussion. Thanks are also given to Singapore–Massachusetts Institute of Technology (MIT) Alliance for the financial support.

References

[1] X. Yang, J.B. Heroux, M.J. Jurkovic, W.I. Wang, Appl. Phys. Lett. 76 (2000) 795.
[2] M. Telford, III-Vs Rev. 14 (2001) 28.
[3] W.G. Bi, C.W. Tu, Appl. Phys. Lett. 70 (1997) 1608.
[4] A.Yu. Egorov, D. Bernklau, B. Borchert, S. Illek, D. Livshits, A. Rucki, M. Schuster, A. Kaschner, A. Hoffmann, Gh. Dumitras, M.C. Amann, H. Riechert, J. Crystal Growth 227–228 (2001) 545.
[5] I. Vurgaftman, J.R. Meyer, L.R. Ram-Mohan, J. Appl. Phys. 89 (2001) 5815.
[6] M.-A. Pinault, E. Tournie, Appl. Phys. Lett. 78 (2001) 1562.
[7] S.Z. Wang, S.W. Xie, Q.J. Pang, H. Zheng, Y.X. Xia, R.B. Ji, Y. Wu, L. He, Z.M. Zhu, G.H. Li, Z.P. Wang, J. Crystal Growth 220 (2000) 548.
[8] S.C. Jain, M. Willander, J. Narayan, R. Van Overstraeten, J. Appl. Phys. 87 (2000) 965.
[9] A. Kaschner, T. Luttgert, H. Born, A. Hoffmann, A.Yu. Egorov, H. Riechert, Appl. Phys. Lett. 78 (2001) 1391.
[10] L. Grenouillet, C. Bru-Chevallier, G. Guillot, P. Gilet, P. Duvaut, C. Vannuffel, A. Million, A. Chenevas-Paule, Appl. Phys. Lett. 76 (2000) 2241.
[11] M. Colocci, M. Gurioli, A. Vinattieri, J. Appl. Phys. 68 (1990) 2809.
[12] S.Z. Wang, S.F. Yoon, T.K. Ng, W.K. Loke, W.J. Fan, J. Crystal Growth 242 (2002) 87.
[13] W.J. Fan, S.F. Yoon, T.K. Ng, S.Z. Wang, W.K. Loke, R. Liu, A. Wee, Appl. Phys. Lett. 80 (2002) 4136.
[14] D. Ouadjaout, Y. Marfaing, Phys. Rev. B 41 (1990) 12096.
[15] R. Hill, J. Phys. C: Solid State Phys. 7 (1974) 521.
[16] W.K. Loke, S.F. Yoon, S.Z. Wang, T.K. Ng, W.J. Fan, J. Appl. Phys. 91 (2002) 4900.
[17] W.Z. Shen, H.Z. Wu, P.J. McCann, J. Appl. Phys. 91 (2002) 3621.